Transverse effects in the production of x rays with a free-electron laser based on an optical undulator

A. Bacci,[1] M. Ferrario,[3] C. Maroli,[2] V. Petrillo,[2] and L. Serafini[1]

[1]*INFN-Sezione di Milano, Via Celoria 16, 20133 Milano, Italy*

[2]*Dipartimento di Fisica dell'Università di Milano e INFN-Sezione di Milano, Via Celoria 16, 20133 Milano, Italy*

[3]*INFN-LNF, Via Fermi 40, 00044 Frascati (RM), Italy*

(Received 25 January 2006; published 27 June 2006)

The interaction between high-brilliance electron beams and counterpropagating laser pulses produces x rays via Thomson backscattering. If the laser source is long and intense enough, the electrons of the beam can bunch on the scale of the emitted x-ray wavelength and a regime of collective effects can establish. In this case of dominating collective effects, the FEL instability can develop and the system behaves like a free-electron laser based on an optical undulator. Coherent x rays can be irradiated, with a bandwidth very much thinner than that of the corresponding incoherent emission. The emittance of the electron beam and the distribution nonuniformity of the laser energy are the principal quantities that limit the growth of the x-ray signal. In this work we analyze with a 3D code the transverse effects in the emission produced by a relativistic electron beam when it is under the action of an optical laser pulse and the x-ray spectra obtained. The scalings typical of the optical wiggler, characterized by very short gain lengths and overall time durations of the process, make possible considerable emission also in violation of the Pellegrini criterion for static wigglers. A generalized form of this criterion is validated on the basis of the numerical evidence.

DOI: 10.1103/PhysRevSTAB.9.060704 PACS numbers: 41.60.Cr, 41.20.−q

I. INTRODUCTION

A Thomson backscattering setup can be considered in principle as a source of intense x-ray pulses which is at the same time easily tunable and highly monochromatic. Because of recent technological developments in the production of high-brilliance electron beams and high power CPA laser pulses, it is now even conceivable to make steps toward their practical realization [1–6].

The radiation generated in the Thomson backscattering is usually considered incoherent and calculated by summing at the collector the intensities of the fields produced in single processes by each electron [7–13]. If the laser pulse is long enough, however, collective effects can establish and become dominant. The system in this range of parameters behaves therefore like a free-electron laser, where the static wiggler is substituted by the optical laser pulse [14–17].

From the point of view of the theoretical description of the process, the possibility of generate coherent x radiation can be demonstrated with the same set of one-dimensional equations that are used in the theory of high-gain free-electron laser amplifier [18,19]. This set of 1D equations gives a simple but clear description of the growth of the radiation on the electron bunch during its interaction with the laser pulse. However, many aspects of the process are connected with the finite transverse geometry of the electron beam and of the laser and, in order to give a quantitative evaluation of the radiation pulses, it is obviously necessary to consider 3D equations.

In this paper, we write and solve a system of 3D equations that describes the coherent growth of the radiation in the laser-beam interaction. In particular, in Sec. II we recall the derivation of such a system. A set of numerical results relevant to a case of practical interest, with a discussion of their importance, will be given in Sec. III. The conclusions are presented in Sec. IV.

II. 3D EQUATIONS

We start from the Maxwell-Lorentz equations that describe both laser and collective electromagnetic fields and from the relativistic equations of motion for the electrons of the beam. The laser and collective fields are given in terms of the corresponding scalar and vector potentials in the Coulomb gauge.

We assume that the laser is circularly polarized with the following form of the vector potential $\mathbf{A}_L$ (the laser pulse propagates along the z-axis in the negative direction):

$$\mathbf{A}_L(xyzt) = \frac{a_{L0}}{\sqrt{2}}[g(xyzt)e^{-i(k_L z+\omega_L t)}\hat{\mathbf{e}} + cc] + O\left(\frac{\lambda_L}{\sigma_L}\right), \quad (1)$$

where $\lambda_L = 2\pi/k_L$ is the laser wavelength, σ_L the rms laser spot radius averaged on the laser intensity, $\omega_L = ck_L$ the angular frequency, and $\hat{\mathbf{e}} = \frac{1}{\sqrt{2}}(\mathbf{e}_x + i\mathbf{e}_y)$. The envelope $g(xyzt)$ is considered to be a slowly varying function of all variables xyz and t and is defined as a complex number with $|g(xyzt)| \leq 1$. In the case, for instance, of a laser pulse with a Gaussian transverse shape, the envelope has the form [20]

$$g(xyzt) = \Phi(z + ct)\frac{1 + i\frac{z}{Z_0}}{1 + \frac{z^2}{Z_0^2}} \exp\Big[- \frac{x^2 + y^2}{2\sigma_L^2(1 + \frac{z^2}{Z_0^2})} - i\frac{x^2 + y^2}{2\sigma_L^2(\frac{z}{Z_0} + \frac{Z_0}{z})}\Big], \quad (2)$$

where $Z_0 = 2\pi{\sigma_L}^2/\lambda_L$ is the Rayleigh length and the form of the (real) function Φ [with $0 \le \Phi(z) \le 1$] depends on the shape of the pulse along the z-axis. Notice that $\mathbf{A}_L$ is perpendicular to the z-axis up to terms of the order of λ_L/σ_L, which is consistent with the gauge requirement $\nabla \cdot \mathbf{A}_L = 0$. Another interesting case is when the laser pulse is guided with a profile $g(x, y, z, t)$ described by a step function of radius w_0.

We make at this point the basic assumption that the collective scalar and vector potentials $\varphi(xyzt)$ and $\mathbf{A}(xyzt)$ have a slow dependence on the transverse space variables x and y, i.e., that they vary on a transverse scale L_T much greater than the radiation wavelength $\lambda = 2\pi/k$ and write, accordingly to the single-mode hypothesis frequently used in 1D treatments,

$$\begin{aligned}\mathbf{A}\,(xyzt) &= M(xyzt)\hat{\mathbf{e}} + cc + O(\lambda/L_T) \\ &= A(xyzt)e^{i(kz-\omega t)}\hat{\mathbf{e}} + cc + O(\lambda/L_T), \end{aligned} \quad (3)$$

where $M(xyzt) = A(xyzt)e^{i(kz-\omega t)}$ and $\omega = ck$ is the radiation angular frequency. As in Eq. (1), the amplitude $A(xyzt)$ will therefore be considered as a slowly varying function of all variables xyz and t and the collective potential $\mathbf{A}$ is perpendicular to the z-axis up to terms of the order of λ/L_T.

We write the relativistic equation of motion of each electron in the form

$$\frac{d\mathit{\Pi}_j(t)}{dt} = e\{\nabla[\varphi - \beta_j(t) \cdot (\mathbf{A}_L + \mathbf{A})]\}_{\mathbf{x}=\mathbf{r}_j(t)}, \quad (4)$$

with $\mathbf{r}_j(t)$ the instantaneous position of the electron, $\mathbf{\Pi}_j(t) = \boldsymbol{\pi}_j(t) - (e/c)(\mathbf{A}_L + \mathbf{A})_{\mathbf{x}=\mathbf{r}_j(t)}$ the generalized momentum, and $\boldsymbol{\pi}_j(t) = mc\mathbf{p}_j(t)$ the mechanical momentum in which we use the definition

$$\mathbf{p}_j(t) = \gamma_j(t)\boldsymbol{\beta}_j(t). \quad (5)$$

By projecting Eq. (4) on the plane transverse to the z-axis, we see that $\mathit{\Pi}_{j\perp}$ is a constant of the motion to dominant order in the small parameters and as is usually done in 1D treatments we shall even assume that $\mathit{\Pi}_{j\perp} = 0$ always to dominant order, which leads to the equation

$$\beta_{j\perp}(t) = \frac{e}{mc^2\gamma_j(t)}(\mathbf{A}_L + \mathbf{A})_{\mathbf{x}=\mathbf{r}_j(t)} + \cdots. \quad (6)$$

Here and in all following equations, the dots in the right-hand side (rhs) stand for terms that are smaller than those explicitly written at the left and that can be disregarded in the limit in which the parameters of smallness go to zero.

By inserting (6) into (4) and neglecting all terms containing the collective scalar potential φ (''space charge'' effects), one has

$$\frac{d\mathit{\Pi}_j(t)}{dt} = -\frac{e^2}{2mc^2\gamma_j(t)}[\nabla(\mathbf{A}_L + \mathbf{A})^2]_{\mathbf{x}=\mathbf{r}_j(t)} + \cdots. \quad (7)$$

where

$$(\mathbf{A}_L + \mathbf{A})^2 = a_{L0}^2|g|^2 + 2|A|^2 + 2\sqrt{2}a_{L0}\,\mathrm{Re}(g^*Ae^{i\theta}) + \cdots. \quad (8)$$

$\theta = (k + k_L)z + c(k_L - k)t$ and the term $2|A|^2$ on the rhs of (8) is usually omitted.

The axial motion of the single particle is obtained by projecting Eq. (7) on the z-axis and using (5) and (8), which gives

$$\begin{aligned}\frac{dp_{jz}(t)}{dt} = &-\frac{e^2}{2m^2c^3\gamma_j(t)}\Big\{a_{L0}^2\Big[\frac{\partial}{\partial z}|g|^2\Big]_{\mathbf{x}=\mathbf{r}_j(t)} \\ &- 2\sqrt{2}(k + k_L)a_{L0}\,\mathrm{Im}[(g^*A)_{\mathbf{x}=\mathbf{r}_j(t)}e^{i\theta_j(t)}]\Big\} \\ &+ \cdots, \end{aligned} \quad (9)$$

where the phase angles $\theta_j(t)$ of the particles in the combined laser plus collective field are given by

$$\theta_j(t) = (k_L + k)z_j(t) + c(k_L - k)t. \quad (10)$$

The first term on the rhs of Eq. (9) gives the ponderomotive force exerted on the electron as it enters or leaves the laser pulse, while the second term is due to the action of all other electrons of the beam and is therefore responsible for collective effects and, in particular, the free-electron laser (FEL) instability.

The transverse motion is likewise obtained by projecting Eq. (7) on the x, y plane which gives

$$\begin{aligned}mc\frac{d\mathbf{p}_{j\perp}(t)}{dt} = &\frac{e}{c}\frac{d}{dt}[(\mathbf{A}_L + \mathbf{A})_{\mathbf{x}=\mathbf{r}_j(t)}] \\ &- \frac{e^2}{2mc^2\gamma_j(t)}\{\nabla_\perp(a_{L0}^2|g|^2 + 2\sqrt{2}a_{L0} \\ &\times \mathrm{Re}(g^*\tilde{A}e^{i\theta})\}_{\mathbf{x}=\mathbf{r}_j(t)} + \cdots. \end{aligned}$$

Omitting rapidly varying terms by simply taking the mean value of both sides of this equation over the laser period, one obtains finally

$$\begin{aligned}\frac{d\mathbf{p}_{j\perp}(t)}{dt} = &-\frac{e^2}{2m^2c^3\gamma_j(t)}\{a_{L0}^2(\nabla_\perp|g|^2)_{\mathbf{x}=\mathbf{r}_j(t)} \\ &+ 2\sqrt{2}a_{L0}\,\mathrm{Re}[(\nabla_\perp(g^*A))_{\mathbf{x}=\mathbf{r}_j(t)}e^{i\theta_j(t)}]\} + \cdots. \end{aligned} \quad (11)$$

As in Eq. (9), the first term to the right of (11) gives the ponderomotive focusing or defocusing actions due to the laser transverse gradients while the second term takes into

account collective contributions to the transverse motion. Notice also that, due to the assumed slow dependence on both x and y, this last term is smaller than the corresponding term on the rhs of Eq. (9).

The last point consists in the derivation of an approximate equation for the collective vector potential $\mathbf{A}(xyzt)$ directly from the Maxwell equation

$$\left(\frac{\partial^2}{\partial t^2} - c^2\nabla^2\right)\mathbf{A}(xyzt) = 4\pi c\mathbf{J}_b - c\frac{\partial}{\partial t}\nabla\varphi,$$

where the beam current density is taken in its microscopic form, i.e., $\mathbf{J}_b = -ec\sum_j \beta_j(t)\delta[\mathbf{x} - \mathbf{r}_j(t)]$, the integer j running from 1 to N, the total number of electrons of the beam. By dropping, as we have already said, the contribution from the scalar potential φ, remembering that $\mathbf{A}$ is to dominant order perpendicular to the z-axis and using again Eq. (6), we write

$$\left(\frac{\partial^2}{\partial t^2} - c^2\nabla^2\right)\mathbf{A}(xyzt) = -\frac{4\pi e^2}{m}\sum_j \frac{1}{\gamma_j(t)} \times (\mathbf{A}_L + \mathbf{A})\delta[\mathbf{x} - \mathbf{r}_j(t)] + \cdots.$$

We neglect $\mathbf{A}$ with respect to $\mathbf{A}_L$ in the driving term of this equation and take definitions (1) and (3) into account to obtain the form

$$\left(\frac{\partial^2}{\partial t^2} - c^2\frac{\partial^2}{\partial z^2}\right)M(xyzt) = c^2\nabla_\perp^2 M - \frac{\omega_b^2 a_{L0}}{\sqrt{2}}\frac{V_b}{N}\sum_j \frac{g(xyzt)}{\gamma_j(t)}e^{-i(k_L z + ck_L t)}\delta[\mathbf{x} - \mathbf{r}_j(t)] + \cdots, \tag{12}$$

where ${\omega_b}^2 = 4\pi e^2 n_b/m$, $n_b = N/V_b$ being the average value of the beam volume density (V_b is the initial volume of the beam).

By using a time scaling procedure, secular terms in the perturbation treatment can be avoided by imposing that the amplitude A is a solution of the following equation:

$$\left(\frac{\partial}{\partial t} + c\frac{\partial}{\partial z}\right)A(xyzt) - i\frac{c}{2k}\nabla_\perp^2 A = -i\frac{\omega_b^2 a_{L0}}{2\sqrt{2}ck}\frac{V_b}{N}\sum_j \frac{g[\mathbf{r}_j(t), t]}{\gamma_j(t)}e^{-i\theta_j(t)}\delta[\mathbf{x} - \mathbf{r}_j(t)] + \cdots.$$

As a final step, taking a continuous average of both sides of this equation over a specified volume V_m, to eliminate the delta functions and change from a microscopic to a macroscopic collective field concept, we may give the equation in its final form:

$$\left(\frac{\partial}{\partial t} + c\frac{\partial}{\partial z}\right)A(xyzt) - i\frac{c}{2k}\nabla_\perp^2 A = -i\frac{\omega_b^2 a_{L0}}{2\sqrt{2}ck}\frac{V_b}{V_b(t)}\frac{1}{N_s}\sum_s \frac{g[\mathbf{r}_s(t), t]}{\gamma_s(t)}e^{-i\theta_s(t)} + \cdots, \tag{13}$$

where $V_b(t)$ is the volume of the beam at time t.

This equation, obtained for the static wiggler by Scharlemann [21], shows the typical driving ("bunching") factor

$$b(xyzt) = \frac{1}{N_s}\sum_s \frac{g[\mathbf{r}_s(t), t]}{\gamma_s(t)}e^{-i\theta_s(t)}, \tag{14}$$

which is similar to that appearing in the 1D version of the theory. The phase angles $\theta_s(t)$ have already been defined in (10), while the integer s in both Eqs. (13) and (14) runs over all values of j for which at the particular time t and point $\mathbf{x}(xyz)$

$$r_j = \sqrt{[x - x_j(t)]^2 + [y - y_j(t)]^2 + [z - z_j(t)]^2} < R_m$$

if we choose, for instance, V_m as a sphere with radius R_m. $N_s(xyzt)$ is the number of electrons that satisfy the preceding inequality.

Equations (9), (11), and (13) are our basic equations. Once restated using the traditional nondimensional variables $\bar{t} = 2\rho\omega_L t$ and $\bar{\mathbf{x}} = 2\rho k_L \mathbf{x}$, they may be summarized as follows:

$$\frac{d}{d\bar{t}}\bar{\mathbf{r}}_j(\bar{t}) = \rho\frac{\mathbf{P}_j(\bar{t})}{\bar{\gamma}_j(\bar{t})}, \tag{15}$$

$$\frac{d}{d\bar{t}}P_{jz}(\bar{t}) = -\frac{\bar{a}_{L0}^2}{2\rho\gamma_0^2}\frac{1}{\bar{\gamma}_j}\left[\frac{\partial}{\partial\bar{z}}|g|^2\right]_{\bar{\mathbf{x}}=\bar{\mathbf{r}}_j} - \frac{2}{\bar{\gamma}_j}\mathrm{Re}[(g^*\bar{A})_{\bar{\mathbf{x}}=\bar{\mathbf{r}}_j}e^{i\theta_j(\bar{t})}] + \cdots \tag{16}$$

$$\frac{d}{d\bar{t}}\mathbf{P}_{j\perp}(\bar{t}) = -\frac{\bar{a}_{L0}^2}{2\rho\gamma_0^2}\frac{1}{\bar{\gamma}_j}[\bar{\nabla}_\perp|g|^2]_{\bar{\mathbf{x}}=\bar{\mathbf{r}}_j} - \frac{4\eta}{1+\frac{k_L}{k}} \times \frac{1}{\bar{\gamma}_j}\mathrm{Im}\{[\nabla_\perp(g^*\bar{A})]_{\bar{\mathbf{x}}=\bar{\mathbf{r}}_j}e^{i\theta_j(\bar{t})}\} + \ldots., \tag{17}$$

$$\left(\frac{\partial}{\partial\bar{t}}+\frac{\partial}{\partial\bar{z}}\right)\bar{A}(\bar{\mathbf{x}},\bar{t})-i\eta\bar{\nabla}_{\perp}^{2}\bar{A}=b=\frac{1}{N_S}\frac{V_b}{V_b(t)}\sum_{S}\frac{g[\bar{\mathbf{r}}_S(\bar{t}),\bar{t}]}{\bar{\gamma}_S(\bar{t})}e^{-i\theta_S(\bar{t})}+\cdots, \tag{18}$$

with the phase angles written in nondimensional form as

$$\theta_j(\bar{t})=\frac{k}{2\rho k_L}\left[\left(1+\frac{k_L}{k}\right)\bar{z}_j(\bar{t})+\left(\frac{k_L}{k}-1\right)\bar{t}\right] \tag{19}$$

and

$$\gamma_j^2=1+\gamma_0^2\rho^2P_{jz}^2+\bar{a}_{L0}^2(|g|^2)_{\bar{\mathbf{x}}=\bar{\mathbf{r}}_j(\bar{t})}+\cdots. \tag{20}$$

In the preceding equations γ_0 is the average value of γ over all electrons of the beam at $t=0$, $\bar{\gamma}_j=\gamma_j/\gamma_0$, $\mathbf{P}_j=\mathbf{p}_j/\gamma_0\rho$, where $\bar{a}_{L0}=\frac{e}{mc^2}a_{L0}$ is the laser parameter,

$$\eta=\frac{k_L}{k}\rho, \tag{21}$$

$$\frac{eA}{mc^2}=-i\left(\frac{\omega_{L0}^2\bar{a}_{L0}}{4\sqrt{2}\omega\omega_L\gamma_0\rho}\right)\bar{A} \tag{22}$$

and the FEL parameter

$$\rho=\frac{1}{\gamma_0}\left[\frac{\omega_b^2\bar{a}_{L0}^2}{16\omega_L^2}\left(1+\frac{\omega_L}{\omega}\right)\right]^{1/3}. \tag{23}$$

The resonant frequency turns out to have the usual expression $k\approx(4\gamma_0^2k_L)/(1+\bar{a}_{L0}^2)$, adopted in most 1D treatments. Furthermore we can note that, in the same way as in the theory of the static wiggler, there exists another resonance at a lower frequency, that, in this case, coincides with the frequency of the laser. This fact can contribute to eliminate the spiking character of the signal.

III. NUMERICAL RESULTS AND DISCUSSION

We have developed a three-dimensional code that solves the set of Eqs. (15)–(18), based on a fourth-order Runge-Kutta for the particles and on a finite-difference scheme for the radiation field. As a first example of solution, we have chosen the following case: the laser is counterpropagating with respect to the electron bunch and has a wavelength $\lambda_L=10\ \mu$m, as in the case of a CO_2 device. Typical maximum powers of these lasers are of the order 40–100 GW, corresponding to a total energy ranging in the interval 4–10 J for a time duration of the pulse of 100 ps. The rms radius of the laser focal spot σ_L can range from forty to a few hundreds μm with a laser parameter $\bar{a}_{L0}$ varying consequently. A narrow band of frequencies around the nominal resonance has been analyzed.

The bunch of electrons we have considered first is similar to the typical Sparc-PlasmonX case [22], with an average value of γ, $\langle\gamma\rangle=60$, corresponding to an energy of 30 MeV. This value of $\langle\gamma\rangle$ leads to a resonant wavelength $\lambda=7.56$Å, in the range of the soft x rays. The dimensions of the electron packet are: 1 mm of length, an average initial radius σ_0 of 25 μm and the total charge is 1–5 nC, giving a current in the range 0.3–1.5 kA. A momentum spread $\Delta p_z/p_z$ of about 10^{-4} has been assumed. The initial radial normalized emittance ε_n has been varied from 0 up to about 2 μm, because the lowest values of emittance obtained experimentally for a beam of 1 nC are around or at least slightly under the value of 1.5 mm mrad [23,24].

In the case shown in Fig. 1, the electron beam, of charge 3 nC and 1 mm long, has a current of 0.9 kA, so that the Pierce parameter ρ is $\rho=2.81\times10^{-4}$, corresponding to a gain length of about $L_g=2.83$ mm. The quantum parameter q [25] is 0.19.

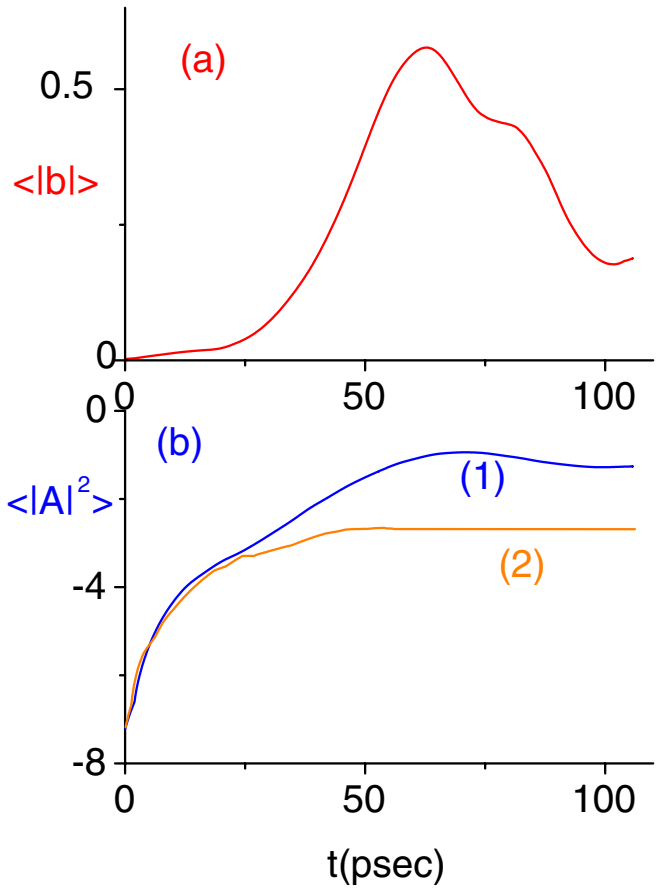

FIG. 1. (Color) (a) average bunching $\langle|b|\rangle$ in the middle of the bunch vs time, (b) logarithmic plot of $\langle|A|^2\rangle$ vs time in picoseconds in the (1) coherent and (2) incoherent case. In the calculation $w_0=50\ \mu$m with a flat laser profile, $\bar{a}_{L0}=0.3$, $Q=3$ nC, $I=0.9$ kA,$\langle\gamma\rangle=60$, $\Delta p_z/p_z=10^{-4}$, $\varepsilon_n=0.6\ \mu$m, $\Delta\omega/\omega=-10^{-4}$.

The laser pulse has been considered flat both transversally and along z, with a power of 100 GW, and a laser focal spot with radius $w_0 = 50\ \mu$m ($\bar{a}_{L0} = 0.3$). This distribution of energy can be obtained by guiding the laser beam, and it is necessary in the case of these parameters because, assuming a Gaussian distribution, the Rayleigh length of the laser beam would be $Z_0 = 785\ \mu$m, shorter than the gain length, thereby impeding the development of the instability. Figure 1 shows the typical growth of the collective potential amplitude in time [window (b), curve (l)], as well as the bunching factor [window (a)]. The amplitude of the vector potential $\langle |A|^2 \rangle$ in the figure has been calculated in the middle of the electron bunch at a position $z = \langle z \rangle$ and averaged on the transverse plane. Other values chosen in this case are: a value of the transverse normalized emittance $\varepsilon_n = 0.6$ mm mrad, $\Delta\gamma/\gamma = 10^{-4}$, and $\Delta\omega/\omega = -10^{-4}$. Moreover, the laser beam has been maintained up to the saturation of the radiation. The graphs show that the collective effects appear after 40 ps, and the signal saturates in a total of 8 gain lengths, corresponding to about 80 ps. In this curve is also reported the incoherent signal [window (b), curve (2)], obtained neglecting the collective field in the motion equations.

The radiated photons collected on a transverse section can be evaluated in terms of the electromagnetic energy flux:

$$\frac{dN}{d\Sigma} = \frac{1}{\hbar\omega_R}\frac{dW}{d\Sigma} = \frac{\omega_R}{2\pi c\hbar}\int_{-\infty}^{+\infty} dt |A_{\rm fis}|^2 \qquad (24)$$

that, using the nondimensional units, becomes

$$\frac{dN}{d\Sigma} = \frac{n_0 mc^3\gamma}{2\hbar\omega_L}\int_{-\infty}^{\infty} d\bar{t}\,|\bar{A}(z_{\rm coll}, t)|^2. \qquad (25)$$

In the case of Fig. 1, the saturation level of the radiation is $\langle |A|^2 \rangle_{\rm peak} = 0.11$, which corresponds to a total photon number of 2.36×10^{10}, while the incoherent process produces 2 orders of magnitude less photons.

Figure 2 gives the level curves of the potential amplitude $|A|^2$ in a transverse plane x, y in the electron frame in the middle of the electron beam $\langle z \rangle$ at various times for the same case as Fig. 1.

After the initial phase where the signal appears chaotic [windows (a) and (b) at 15 and 45 ps], the signal cleans up during the exponentiation [(c) at 75 ps] and reaches finally a smooth shape during or after the saturation phase [(d) at 105 ps].

The transverse increase of the radiation spot is initially due to the divergence of the electron beam, regulated by the law $\sigma = \sigma_0\sqrt{1 + z^2/\beta^{*2}}$, with $\beta^* = (\sigma_0^2/\varepsilon_n)\gamma = 61$ mm. The Rayleigh length of the radiation $Z_R = 2\pi\sigma_R^2/\lambda = 2.59$ m is in fact very much larger than the gain length L_g so that the radiation diffraction can be neglected. This can also be seen from the scaled

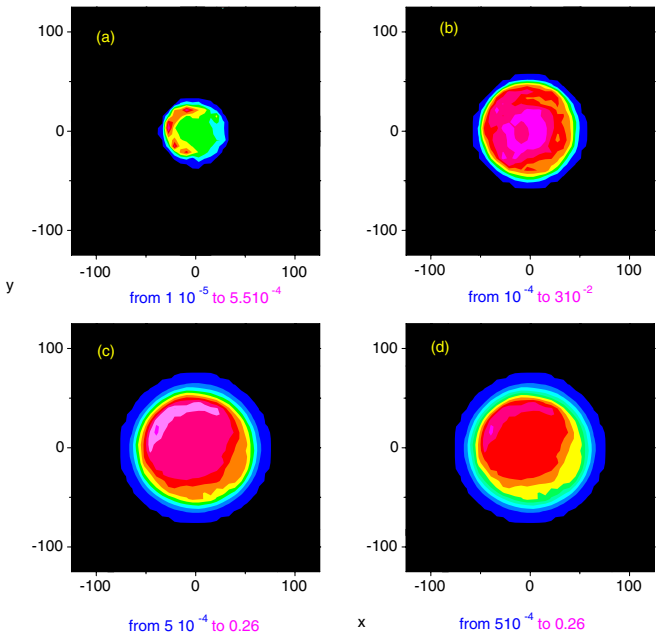

FIG. 2. (Color) Level curves of $|A|^2$ in the (x, y) plane for the same parameters of Fig. 1 and (a) $t = 15$ ps, (b) $t = 45$ ps, (c) $t = 75$ ps, and (d) $t = 105$ ps.

Eqs. (17) and (18), where the very small parameter η defined in Eq. (21) multiplies respectively the collective term in the transverse momentum equation and the diffraction term in the wave equation. In a second stage, if the beam radius becomes larger than the laser spot radius the radiation tends to remain concentrated inside the interaction region.

In Fig. 3 the spectrum of the signal is represented in the case of $\varepsilon_n = 0.6\ \mu$m versus the quantity $\Delta\omega/(\omega\rho)$, so that this graph gives immediately the bandwidth in terms of ρ.

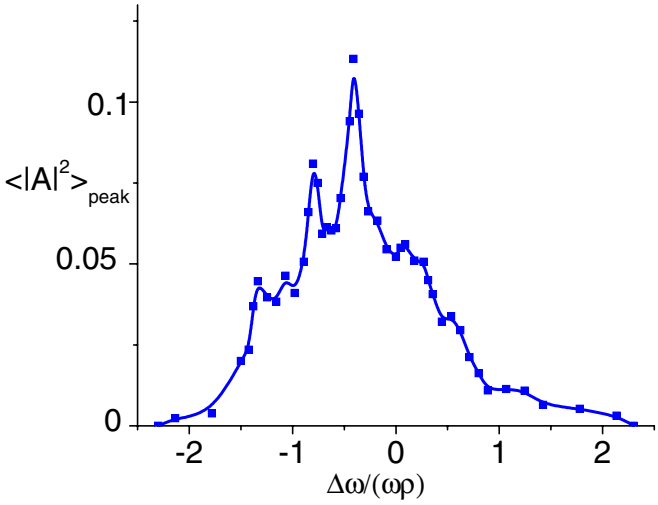

FIG. 3. (Color) First peak value of $\langle |A|^2 \rangle$ versus $\Delta\omega/(\omega\rho)$ for parameters similar to those of Fig. 1.

The spectrum presents a sequence of spikes and its width is few times ρ.

For large negative detunings, the signal grows in a longer time.

In Fig. 4 the dependence of the peak value of the intensity on the transverse emittance is reported in correspondence of the peak in the radiation spectrum occurring at $\Delta\omega/\omega = -10^{-4}$.

The variation of the radiation intensity with the emittance depends on three factors: first, the current density carried by the beam decreases with emittance, causing a lowering in the source factor. Second, when the beam radius exceeds the laser spot size, the decrease of the radiation intensity is due simply to the exit of the more external electrons from the interaction region. Finally, if the laser pulse has transverse and longitudinal profiles, the outer electrons go out from resonance and the instability develops at lower levels or it does not develop at all.

The peak brilliance of the radiated x-ray beam can be calculated as

$$B_{pk} = \frac{N \times 10^{-3}}{\Sigma\tau\frac{\Delta\omega}{\omega}} \text{photons}/(\text{sec mm}^2\,\text{mr}^2\ 0.1\%)$$

where $\Sigma = \varepsilon_n^2/\gamma^2$ is the dominant part of the 4D-phase space area of the photon and electron beams, τ is the whole duration of the bunch and $\Delta\omega/\omega$ is the bandwidth. Assuming $N = 2.36 \times 10^{10}$, $\Delta\omega/\omega = 2\rho = 5.6 \times 10^{-4}$, $\tau = 3$ ps, $\varepsilon_n = 0.6$ mm mrad, $\gamma = 60$, we obtain $B_{pk} = 1.5 \times 10^{26}$, while the coherent power of the source is 2 MW.

As the scientific community is giving strong effort to developing and commissioning facilities aimed to the production of coherent and intense x-ray pulses based on static undulator free-electron lasers, it is interesting to compare the characteristics of the radiation beam obtained in the present calculation with those foreseen, for instance, in the

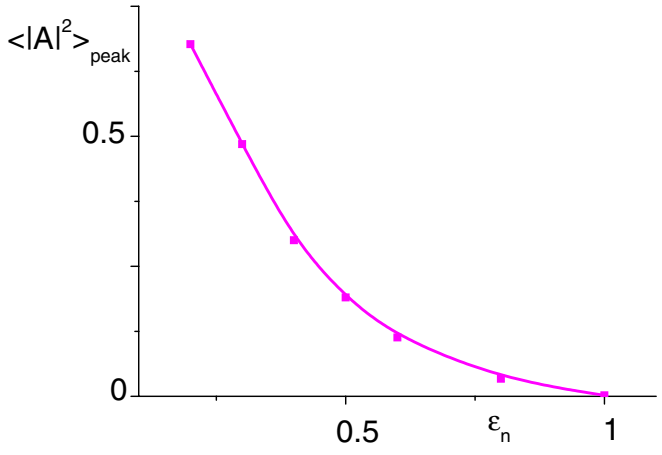

FIG. 4. (Color) $\langle|A|^2\rangle_{\text{peak}}$ versus $\varepsilon_n$evaluated in micron for the same case of Fig. 1 and with $\Delta\omega/\omega = -10^{-4}$, $w_0 = 50$ micron, $a_{L0} = 0.3$, $\Delta\gamma/\gamma = 10^{-4}$.

LCLS and in the TESLA projects [26,27]. In the case of SLAC, the total number of photons per pulse is 2×10^{12}, the calculated peak brilliance is 1.2×10^{33}, while the coherent power is 9 GW for a radiation wavelength of $\lambda = 1.5$ Å. In the case of XFEL the coherent brilliance is estimated 10^{33}, with a photon flux of 10^{12} photons/bunch at 0.1 nm of wavelength.

In conclusion of this first example we note that, as it appears from the data used, the electron bunch adopted is above the present state of the art of the experimental production of high brightness beams for what concerns the values of the transverse emittance.

Another example is provided by a beam with an energy of about 15 MeV (a factor of 2 lower than the typical Sparc-PlasmonX case), corresponding to $\langle\gamma\rangle = 30$, with a mean radius $\sigma_0 = 10$ μm, a total charge of 1 nC, a length $L_b = 200$ μm, corresponding to a beam current of $I = 1.5$ kA. The laser pulse considered in this case has wavelength $\lambda_L = 0.8$ μm. Furthermore, we have assumed a focal spot of radius w_0 of about 50 μm with a laser parameter of $\bar{a}_{L0} = 0.8$ so that the radiation turns out to have $\lambda = 3.64$ Å and the Pierce parameter ρ is 4.38×10^{-4}. With these values the gain length corresponds to about 145 μm, the appearance and the saturation of the collective effects (taking place in 7–12 gain lengths) being contained in 5 picoseconds, a time of the same order of the duration of the laser pulse. The quantum parameter q is 0.5, a rather high value, that can however be justified by recent numerical calculations [28] showing that quantum effects appear appreciably if $\overline{\rho} = 1/q \geq 0.4$.

The energy spread $\Delta\gamma/\gamma$ of the electron beam has been chosen 1×10^{-4} and the initial normalized transverse emittance has been varied from 0 up to 2.

In Fig. 5 the growth of the collective potential amplitude evaluated in the middle of the bunch and averaged on the transverse section is shown in time [window (b), curve (1)], as well as the bunching factor [window (a)]. The parameters of this calculation are: a flat laser profile inside a region with $w_0 = 50$ μm, the laser parameter $\bar{a}_{L0} = 0.8$, a value of the initial emittance of $\varepsilon_n = 0.88$ μm, a detuning of $\Delta\omega/\omega = -2 \times 10^{-4}$.

The saturation level of the radiation is reached at $t = 4$ ps at $\langle|A|^2\rangle_{\text{peak}} = 0.275$, with a total number of photons of 1.86×10^{10}, against the 2×10^8 provided by the incoherent process. The peak brilliance, for this example, is 3.7×10^{25} photons/(s mm^2 mr^2 0.1%), while the coherent power is 15.5 MW.

In Fig. 6 the spectrum of the radiation is reported versus $\Delta\omega/(\omega\rho)$ for (a) $\varepsilon_n = 0.44$ μm and (b) $\varepsilon_n = 0.88$ μm.

We can note an enlargement of a factor of 2 of the bandwidth with increasing emittance.

In Fig. 7 the dependence of the saturation radiation on the emittance is presented. Curve (a) is relevant to the situation of flat laser pulse with $w_0 = 50$ μm, while curve (b) shows the more critical situation where a Gaussian

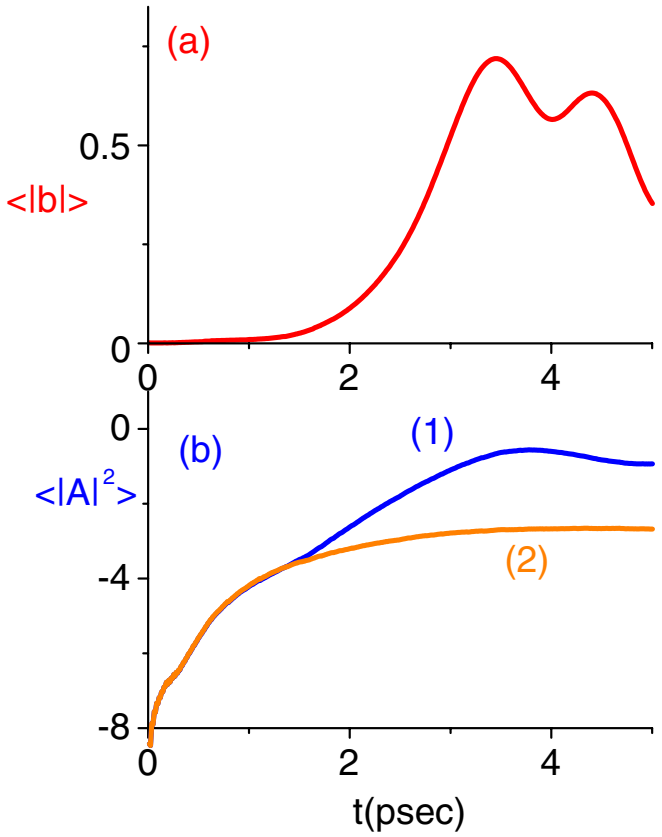

FIG. 5. (Color) Averaged bunching [window (a)] and logarithm of the radiation intensity [window (b)] versus time in the coherent (1) and incoherent (2) case for: $\lambda_L = 0.8\ \mu$m, $\bar{a}_{L0} = 0.8$, $\Delta\gamma/\gamma = 10^{-4}$, $\Delta\omega/\omega = -2 \times 10^{-4}$, $\varepsilon_n = 0.88\ \mu$m.

profile for the laser has been assumed. In this case the quantity σ_L has been taken equal to 106 μm with $\bar{a}_{L0} = 0.8$, increasing consequently the laser power.

We must note that in all situations we have considerable emission in violation of the Pellegrini criterion [29] for a static wiggler. In fact, in case (a) of Fig. 7, for instance, the emittances considered largely exceed the value $\gamma\lambda/4\pi$, that in this case is about $9 \times 10^{-4}\ \mu$m. We can justify this result by considering that the line width in a situation dominated by emittance effects can be written as [30]

$$\frac{\Delta\lambda}{\lambda} \approx \frac{\gamma^2\theta^2}{1 + a_{L0}^2} \approx \frac{\varepsilon_n^2}{\sigma_0^2}. \tag{26}$$

In order to have considerable emission, we must assume that the linewidth $\Delta\lambda/\lambda < \alpha\rho$, with α a numerical factor not very much larger than 1. Hence, we can write for the emittance

$$\varepsilon_n \leq \sqrt{\alpha\rho}\,\sigma_0. \tag{27}$$

Considering the definitions of the gain length $Lg = \lambda_L/(4\pi\rho)$ and that of the radiation Rayleigh length $Z_R = 2\pi\sigma_R^2/\lambda$, we can express the factor ρ in terms of the ratio Z_R/L_g, obtaining $\rho = (Z_R/L_g)[(\lambda\lambda_L)/(8\pi^2\sigma_R^2)]$. Supposing furthermore that the electron beam and the radiation overlap, so that $\sigma_0 = \sigma_R$, and remembering the resonance relation in its simpler expression $\lambda_L = 4\gamma^2\lambda$, we obtain for an optical undulator

$$\varepsilon_n \leq \sqrt{\alpha}\sqrt{\frac{Z_R}{L_g}}\frac{\lambda\gamma}{\sqrt{2}\pi}, \tag{28}$$

where $\alpha = \frac{\delta\omega}{\omega\rho}$. This expression can be obtained in a more formal way following Ref. [31], considering however that with a laser wiggler the trajectories are straight lines and the betatron oscillations are not present. The condition under which the transverse emittance does not affect the gain can be therefore written as

$$\mathrm{Im}\,\Omega \gg p^2/4. \tag{29}$$

Considering that the gain $\mathrm{Im}\Omega$ is $1/(L_g k_L)$ and the transverse momentum p is related to the transverse emittance by

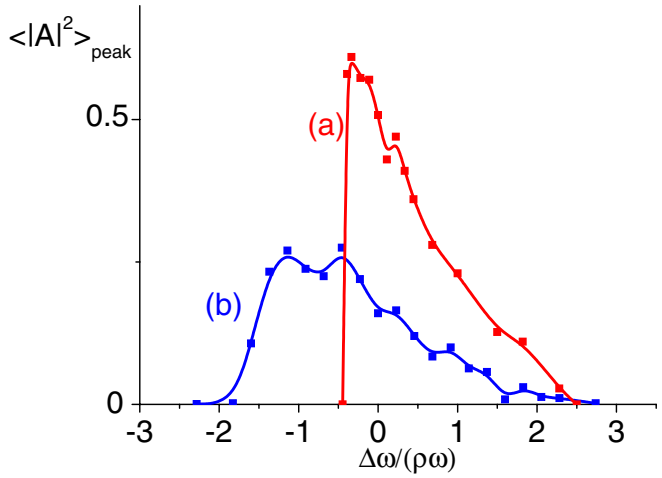

FIG. 6. (Color) $\langle|A|^2\rangle_{\mathrm{peak}}$ versus $\Delta\omega/(\omega\rho)$ for the case of Fig. 5 and (a) $\varepsilon_n = 0.44\ \mu$m and (b) $\varepsilon_n = 0.88\ \mu$m.

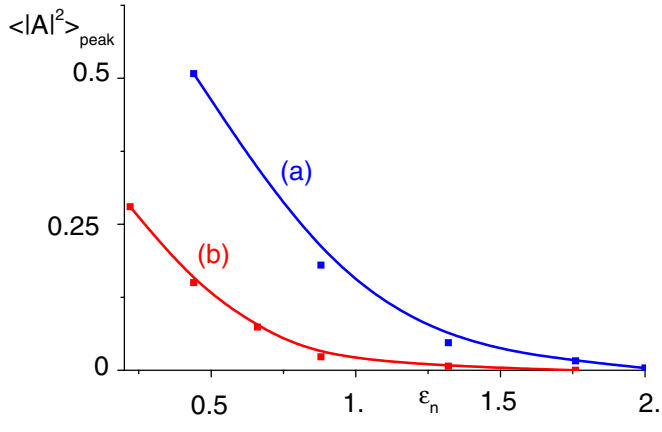

FIG. 7. (Color) $\langle|A|^2\rangle_{\mathrm{peak}}$ versus ε_n for the case of Fig. 5, with $\Delta\omega/\omega = 0$ and for: (a) flat laser profile with $w_0 = 50\ \mu$m and $\bar{a}_{L0} = 0.8$ and (b) Gaussian laser profile with $\bar{a}_{L0} = 0.8$ and $\sigma_L = 106\ \mu$m.

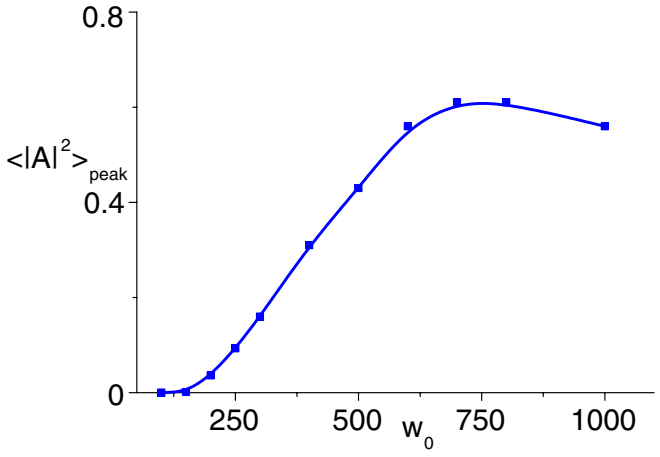

FIG. 8. (Color) $\langle |A|^2 \rangle_{\text{peak}}$ versus w_0 for the case for the Gaussian laser profile for $\varepsilon_n = 0.44\ \mu\text{m}$, $\Delta\omega/\omega = -1 \times 10^{-4}$, $a_{L0} = 0.8$.

the usual definition leading to $\varepsilon_n \approx p\sigma_0$, we can arrange the condition (29) in the same form of (27) a part from a factor of order 1.

The usual Pellegrini criterion can be obtained for a static wiggler assuming $Z_R = L_g$ and considering the resonance condition for the static undulator.

Taking into account the fact that in our situation $Z_R/L_g = 1.18 \times 10^4$, and estimating $\alpha = 2$, we can predict considerable emission up to an emittance value of $\varepsilon_n = 0.3\ \mu\text{m}$ (corresponding to a value of $\varepsilon_{nx} = 0.15$ mm), not far from the results of Fig. 7.

Figure 8 shows the most critical effect, i.e. the dependence of the growth of the signal on the transverse energy distribution of the laser in the case of a Gaussian pulse for $\varepsilon_n = 0.44\ \mu\text{m}$, $\Delta\omega/\omega = -1 \times 10^{-4}$, $\bar{a}_{L0} = 0.8$. In fact, in this case, a spot size with a radius smaller than 75 μm does not permit the onset of the instability. The collective signal in this condition, therefore, does not grow.

A possible remedy could be the development and use of a flat energy distribution of the laser beam obtained with a guided propagation.

This second example is characterized by a choice of the electron beam with larger emittance than in the first case, not far from the best actual experimental values, but with a larger current. However, the requirements on the total energy of the laser and on the stability of the energy transverse profile are in this case particularly demanding.

IV. CONCLUSIONS

We have shown that considerable coherent x-ray radiation is possible as a result of the collective interaction between an electron beam and a counterpropagating laser pulse. The incoherent Thomson backscattering is the first stage of a more complex phenomenon of emission that takes place if the laser pulse is long enough. In this condition in fact the FEL instability can develop and a regime of collective effects can establish. The result is an emission at least 2 order of magnitudes larger than the incoherent one and with a thinner and more peaked spectrum. The characteristics of this x-ray source are, therefore, a substantial improvement with respect to analogous incoherent sources based on the Thomson backscattering. However, the brilliance and the power delivered in these examples are a few orders of magnitude smaller than these same quantities for a static wiggler FEL in the x-ray range.

Other critical issues for the appearance of collective effects are connected with: (i) the current density carried by the electron beam which has to be large enough, (ii) the emittance of the packet which has to be not too much larger than that provided by the generalized Pellegrini criterion, and (iii) the transverse distribution of the laser pulse which cannot have a sensible variation on the region occupied by the electrons. All the data we have shown lead one to conclude that the concrete possibility of developing and constructing a coherent compact x-ray source based on the collective Thomson scattering between a laser and an electron beam is out of the present-day technological state of the art regarding the production of high brightness electron beams and high energy lasers, particularly concerning the values of the electron beam emittance needed and the profile control of the laser energy.

[1] R. W. Schoenlein, W. P. Leemans, A. H. Chin, P. Volfbeyn, T. E. Glover, P. Balling, M. Zolotorev, K. J. Kim, S. Chattopadhyay, and C. V. Shank, Science **274**, 236 (1996).

[2] W. P. Leemans, R. W. Schoenlein, P. Volfbeyn, A. H. Chin, T. E. Glover, P. Balling, M. Zolotorev, K. J. Kim, S. Chattopadhyay, and C. V. Shank, Phys. Rev. Lett. **77**, 4182 (1996).

[3] A. Ting, R. Fischer, A. Fisher, C. I. Moore, B. Hafizi, R. Elton, K. Krushelnick, R. Burris, S. Jadel, K. Evans, J. N. Weaver, P. Sprangle, M. Baine, and S. Ride, Nucl. Instrum. Methods Phys. Res., Sect. A **375**, ABS68 (1996).

[4] I. V. Pogorelsky, I. Ben-Zvi, T. Hirose, S. Kashiwagi, V. Yakimenko, K. Kusche, P. Siddons, J. Skaritka, T. Kumita, A. Tsunemi, T. Omori, J. Urakawa, M. Washio, K. Yokoya, T. Okugi, Y. Liu, P. He, and D. Cline, Phys. Rev. ST Accel. Beams **3**, 090702 (2000).

[5] W. J. Brown, S. G. Anderson, C. P. J. Barty, S. M. Betts, R. Booth, J. K. Crane, R. R. Cross, D. N. Fittinghoff, D. J. Gibson, F. V. Hartemann, E. P. Hartouni, J. Kuba, G. P. Le Sage, D. R. Slaughter, A. M. Tremaine, A. J. Wootton, and P. T. Springer, Phys. Rev. ST Accel. Beams **7**, 060702 (2004).

[6] F. Sakai, A. Endo, S. Ito, K. Takasago, Y. Okada, T. Yanagida, J. Yang, and M. Yorozu, in *Proceedings of Contributed papers. 2001 Particle Accelerator Conference, Chicago, 2001* (IEEE, Piscataway, NJ, 2001), Vol. 4, p. 2695.

[7] J. D. Jackson, *Classical Electrodynamics* (John Wiley and Sons, New York, 1975), p. 679.

[8] E. Esarey, S. K. Ride, and P. Sprangle, Phys. Rev. E **48**, 3003 (1993).
[9] P. Catravas, E. Esarey, and W. P. Leemans, Meas. Sci. Technol. **12**, 1828 (2001).
[10] J. Yang, M. Washio, A. Endo, and T. Hori, Nucl. Instrum. Methods Phys. Res., Sect. A **428**, 556 (1999).
[11] S. Ride, E. Esarey, and M. Baine, Phys. Rev. E **52**, 5425 (1995).
[12] P. Tomassini, A. Giulietti, D. Giulietti, and L. A. Gizzi, Appl. Phys. B **80**, 419 (2005).
[13] K. Lee, B. H. Kim, and D. Kim, Phys. Plasmas **12**, 043107 (2005).
[14] J. Gea-Banacloche, G. T. Moore, R. R. Schlicher, M. O. Scully, and H. Walther, IEEE J. Quantum Electron. **23**, 1558 (1987).
[15] B. G. Danly, G. Bekefi, R. C. Davidson, R. J. Temkin, T. M. Tran, and J. S. Wurtele, IEEE J. Quantum Electron. **23**, 103 (1987).
[16] J. C. Gallardo, R. C. Fernow, R. Palmer, and C. Pellegrini, IEEE J. Quantum Electron. **24**, 1557 (1988).
[17] K. Mima, Y. Kitagawa, T. Akiba, K. Imasaki, S. Kuruma, N. Ohigashi, S. Miyamoto, S. Fujita, S. Nakayama, Y. Tsunawaki, H. Motz, T. Taguchi, S. Nakai, and C. Yamanaka, Nucl. Instrum. Methods Phys. Res., Sect. A **272**, 106 (1988).
[18] W. B. Colson, Phys. Lett. **59A**, 187 (1976).
[19] R. Bonifacio, C. Pellegrini, and L. Narducci, Opt. Commun. **50**, 313 (1984).
[20] M. V. Klein and T. E. Furtak, *Optics* (Wiley, New York, 1987).
[21] E. T. Scharlemann, J. Appl. Phys. **58**, 2154 (1985).
[22] L. Serafini *et al.*, The Project PLASMONX for Plasma Acceleration Experiments and a Thomson X-Ray Source at SPARC, PAC 2005 Knoxville, Tennessee (USA), ID: 2853-TPAE002; L. Serafini *et al.*, Design Study for Advanced Acceleration Experiments and Monochromatic X-ray Production @ SPARC, EPAC2004 Proceedings MOPLT061.
[23] F. Stephan *et al.*, "Recent Results and Perspectives of the Low Emittance Photoinjector at PITZ," Proceedings of the 2004 FEL Conference, pp. 347–350.
[24] F. Zhou, I. Ben-Zvi, M. Babzien, X. Y. Chang, H. Doyuran, R. Malone, X. Y. Wang, and V. Yakimenko, Phys. Rev. ST Accel. Beams **5**, 094203 (2002).
[25] C. B. Schroeder, C. Pellegrini, and P. Chen, Phys. Rev. E **64**, 056502 (2001).
[26] The LCLS Design Study Group, Linac Coherent Light Source (LCLS) Design Study Report (1998).
[27] The European X-Ray Laser Project XFEL, Interim Report of the Scientific and Technical Issue (XFEL-STI) Working Group on a European XFEL Facility in Hamburg (DESY, Germany, 2005).
[28] R. Bonifacio *et al.*, Nucl. Instrum. Methods Phys. Res., Sect. A **543**, 645 (2005).
[29] J. B. Murphy and C. Pellegrini, J. Opt. Soc. Am. B **2**, 259 (1985).
[30] Winthrop J. Brown and Frederic V. Hartemann, Phys. Rev. ST Accel. Beams **7**, 060703 (2004).
[31] Li-Hua Yu and S. Krinsky, Nucl. Instrum. Methods Phys. Res., Sect. A **272**, 436 (1988).